

## Measurement of inclusive photon production cross section with ATLAS

S. CELLA on behalf of the ATLAS COLLABORATION

*CERN - Geneva, Switzerland*

received 29 January 2023

**Summary.** — The cross section for the inclusive production of isolated prompt photons in proton-proton collisions is measured at  $\sqrt{s} = 13$  TeV, using an integrated luminosity of  $139 \text{ fb}^{-1}$  collected with the ATLAS detector at the LHC. The measurement is performed using two criteria for photon isolation: the standard fixed-cone approach and the Frixione isolation prescription. The results show a good agreement with the theoretical predictions within the experimental and theoretical uncertainties. The content of this article is based on my talk at the 108th National Congress of the Italian Physics Society (12th September 2022) and covers the work of my Master's Thesis.

### 1. – Introduction

The ATLAS detector [1] is a multipurpose experiment at the LHC [2]. All of its studies are connected to the interactions of quarks and gluons at large momentum transfers of the colliding particles. Thus, a precise knowledge of the theory underlying these processes, Quantum Chromodynamics (QCD), is fundamental to pursuing the ATLAS physics program. Prompt-photon production in proton-proton ( $pp$ ) collisions provides a testing ground for perturbative QCD (pQCD) in a cleaner environment compared to jet production, since it is less affected by hadronisation effects. Prompt photons are defined as those that are not secondaries from hadron decays. At leading order (LO) in pQCD, two processes contribute to prompt-photon production in  $pp$  collisions: the *direct-photon* processes, in which the photon originates directly from the hard interaction, and the *fragmentation-photon* processes, in which the photon is emitted in the collinear fragmentation of a high transverse momentum parton. This generates a collinear singularity not computable in pQCD. The main background for prompt-photon production in  $pp$  collisions arises from jets containing energetic, light, neutral mesons decaying into an almost collinear photon pair, which carries most of the energy of the jet and can be misidentified as a photon (*fake photon*). Direct photons are generally well separated from the final state hadrons, while fragmentation photons and fake photons are surrounded by hadronic activity. To reduce their contributions, prompt-photon production is studied by requiring the photons to be isolated. Two isolation criteria are considered in this work: the standard *fixed-cone* approach and the *Frixione* isolation prescription [3]. In the first one, a restriction is placed on the amount of transverse energy measured in a cone of fixed

radius  $R_0$  drawn around the photon axis direction:  $E_T^{R_0} < c \cdot p_T^\gamma + E_T^{\text{thres}}$ , where  $p_T^\gamma$  is the photon transverse momentum,  $c$  is a positive constant, and  $E_T^{\text{thres}}$  is a threshold energy value. The drawback of this method is that it leaves a dependence of the cross section on the fragmentation component. The Frixione isolation prescription, instead, allows to reduce to zero the fragmentation contribution, thus providing a cross section which depends only on the direct processes. In this case, the amount of transverse energy inside all the cones of radius  $R < R_0$  is required to be less than a continuous function  $f = f(R)$ , which is required to vanish when  $R$  approaches zero. The continuous version of the criterion is not experimentally applicable, due to the finite size of the photon showers in the calorimeters and the granularity of the detector. Thus, it is necessary to use a discretised version [4], based on a finite set of nested cones, that imposes a restriction on the amount of transverse energy found in each cone,  $E_T^{R_j} < \epsilon_S p_T^\gamma [(1 - \cos R_j)/(1 - \cos R_0)]^n$ , where  $\epsilon_S$  and  $n$  are arbitrary, positive constants. This discretised version is proven to still provide good suppression of the fragmentation contribution. The differential cross section as a function of  $p_T^\gamma$  is measured for  $20 \text{ GeV} < p_T^\gamma < 140 \text{ GeV}$ , using the fixed-cone approach (“Standard analysis”) and the discretised version of the Frixione isolation prescription (“Frixione analysis”) for photon isolation. The aim is to study the feasibility of the use of the Frixione isolation prescription on real data and to test its impact in the reduction of the fragmentation contribution. The low- $p_T^\gamma$  range is chosen since it is the energy interval in which the fragmentation processes give a non-negligible contribution.

## 2. – Cross section measurement procedure

The two analyses are based on  $139 \text{ fb}^{-1}$  of  $pp$  collision data recorded by ATLAS during the entire LHC Run 2 at  $\sqrt{s} = 13 \text{ TeV}$ . Samples of Monte Carlo (MC) events are generated to study the characteristics of signal and background events. Except when noted, the simulated events are passed through a GEANT4 based simulation of the response of the ATLAS detector [5] and reconstructed with the same algorithms as the data [6]. The MC programs PYTHIA 8.186 [7] and SHERPA 2.2.2 [8] (NLO) are used to generate the simulated signal events. The PYTHIA di-jet sample is used to simulate the background of fake photons. The theoretical predictions are computed with the JETPHOX 1.3.1.3 program [9], which includes a full NLO QCD calculation of both the direct and the fragmentation contributions for  $pp \rightarrow \gamma + \text{jet} + X$  processes. A parton-level isolation criterion equal to the one used for data is applied.

The data sample used consists of events selected with a prescaled single-photon trigger with a nominal  $p_T$  threshold of  $10 \text{ GeV}$  and loose photon identification requirements (details on photon identification in [6]). The photon selection described below is applied both to data and to MC samples. Only photon candidates in the kinematic region with  $p_T^\gamma > 20 \text{ GeV}$  and pseudorapidity  $|\eta^\gamma| < 2.37$ , excluding  $1.37 < |\eta^\gamma| < 1.52$ , are considered. The contribution of the fake photons’ background is reduced by selecting photon candidates in a signal region containing tight and isolated photons. The standard analysis uses the fixed-cone approach with parameters  $R_0 = 0.4$ ,  $c = 0.022$  and  $E_{\text{thres}} = 2.45 \text{ GeV}$ . The Frixione analysis uses the discretised version of the Frixione isolation prescription with parameters  $R_0 = 0.4$ ,  $j = 1, 2$ ,  $R_1 = 0.2$ ,  $R_2 = 0.4$ ,  $\epsilon_S = 0.1$ , and  $n = 0.3$ . The values of  $\epsilon_S$  and  $n$  are chosen to obtain an isolation threshold close to the one of the standard analysis. A non-negligible contribution of fake photons remains in the selected sample: it is estimated and subtracted bin-by-bin using the *two-dimensional sideband subtraction method*, a technique described in [10]. The correlation factor,  $R_{\text{bkg}}$ , which accounts for the correlation of the two variables for background events, is extracted

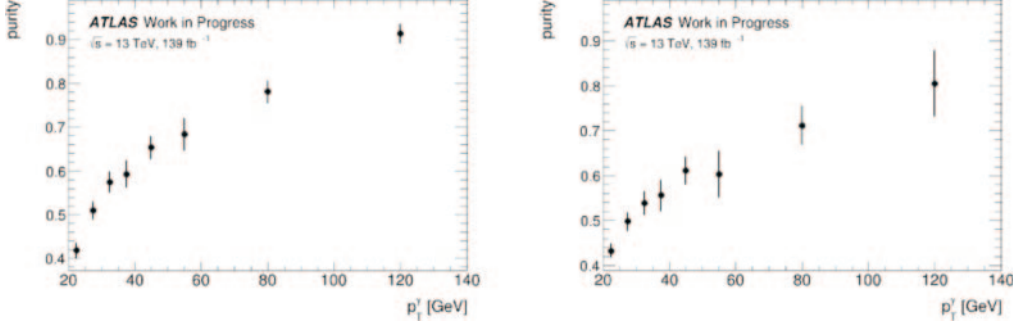


Fig. 1. – Estimated signal purity in data for the standard analysis (on the left) and the Frixione analysis (on the right). The error bars represent the statistical uncertainties.

from the background simulation from the PYTHIA di-jet sample. The fractions of signal events entering the control regions,  $c_K$ , are extracted from the PYTHIA simulation of the signal. Figure 1 shows the signal purity, defined as the number of signal events over the total number of events measured in the signal region. The purity rapidly grows from 42% (43%) to 91% (81%) for the standard (Frixione) analysis, since the jet rejection capability of the detector increases with the candidates'  $p_T$ .

The differential cross section for the bin  $i$  as a function of  $p_T^\gamma$  is computed as the ratio between the number of selected and background-subtracted data events in the bin  $i$  corrected with the *unfolding correction factor*, and the product of the integrated luminosity and the width of the bin  $i$ . The unfolding correction factors are computed using the PYTHIA sample as the ratio of the number of events generated and reconstructed in each bin (*bin-by-bin* unfolding method). They are used to take into account the effects of the detector resolution and inefficiencies, and obtain particle-level kinematic cross section distributions, easier to compare with the theoretical predictions.

The considered sources of systematic uncertainty are the following. The uncertainty on the signal modelling in the MC simulations, which affects the computation of the  $c_K$  factors and the unfolding; another uncertainty on the unfolding procedure is estimated by repeating the analyses using the Bayesian unfolding method [11]. Different sources of systematic uncertainty affect the background subtraction procedure: the dependence of the procedure on the choice of the background control regions is studied by varying the definition of the control regions as described in [10]; uncertainties on  $R_{\text{bkg}}$  and on the signal purity are also considered. Other sources of systematic uncertainty are the modelling of the isolation energy distribution in the MC simulations, the photon identification efficiency, the pile-up reweighting, the photon calibration, and the integrated luminosity measurement. The total systematic uncertainty is computed by adding in quadrature the individual uncertainties. It decreases with  $p_T^\gamma$  from 20% to 5% for the standard analysis, and ranges from 13% to 26% for the Frixione analysis. For both analyses, the systematic uncertainty dominates the statistical uncertainty (always less than 4%) over the full  $p_T^\gamma$  range. The theoretical uncertainties on the JETPHOX predictions are due to terms beyond NLO and to the choice of the PDF set. The total theoretical uncertainty, obtained by adding in quadrature the individual uncertainties, has a value of around 20% over the full  $p_T^\gamma$  interval for both the analyses.

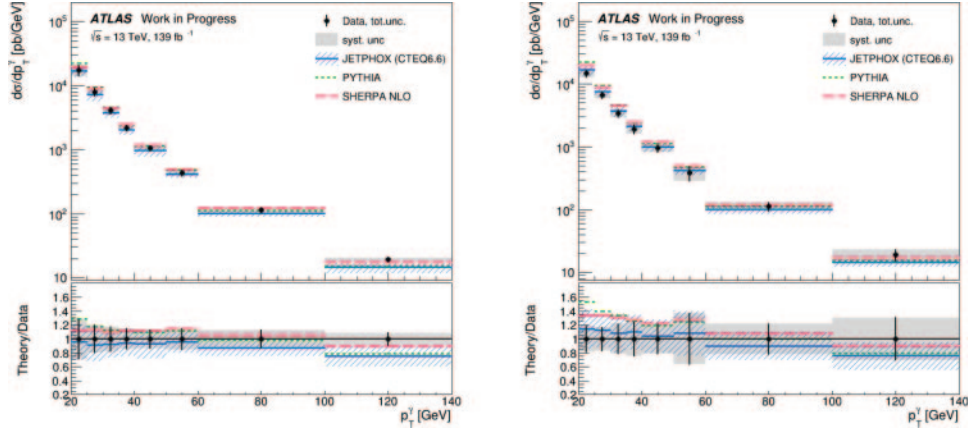


Fig. 2. – Measured cross section for isolated-photon production (dots) as a function of  $p_T^\gamma$ , using the fixed-cone isolation (on the left) and the Frixiene isolation (on the right). The predictions from JETPHOX, PYTHIA, and SHERPA NLO are also shown. The bottom part of the figure shows the ratio of the MC predictions to the measured cross section. The black error bars represent the total uncertainty on data (statistical and systematic uncertainties added in quadrature), while grey squares represent the total systematic uncertainty. The dashed squares represent the theoretical uncertainty on the JETPHOX predictions. Only the statistical uncertainties are shown for PYTHIA and SHERPA NLO.

### 3. – Results

Figure 2 shows the isolated-photon differential cross section as a function of  $p_T^\gamma$  in the 20-140 GeV  $p_T^\gamma$  range, measured using the fixed-cone approach (on the left) and the Frixiene isolation prescription (on the right). The measurements are compared with the NLO JETPHOX predictions: the NLO QCD calculations are consistent with the measurement within the experimental and the theoretical uncertainties. The predictions of PYTHIA and SHERPA NLO are also compared to the measurements: they slightly overestimate the data in the lower  $p_T^\gamma$  bins for the Frixiene analysis. ATLAS publications on inclusive photon cross section measurements use the fixed-cone approach for photon isolation, because of the better experimental precision that can be achieved.

### REFERENCES

- [1] ATLAS COLLABORATION, *JINST*, **3** (2008) S08003.
- [2] EVANS L. and BRYANT P., *JINST*, **3** (2008) S08001.
- [3] FRIXIONE S., *Phys. Lett. B*, **429** (1998) 369.
- [4] BINOTH T. *et al.*, (2010), arXiv:1003.1241, pp. 94–102.
- [5] ATLAS COLLABORATION, *Eur. Phys. J. C*, **70** (2010) 823.
- [6] ATLAS COLLABORATION, *JINST*, **14** (2019) P12006.
- [7] SJÖSTRAND T. *et al.*, *Comput. Phys. Commun.*, **178** (2008) 852.
- [8] GLEISBERG T. *et al.*, *JHEP*, **02** (2009) 007.
- [9] CATANI S. *et al.*, *JHEP*, **05** (2002) 028.
- [10] ATLAS COLLABORATION, *JHEP*, **10** (2019) 203.
- [11] D’AGOSTINI, G., *Nucl. Instrum. Methods A*, **362** (1995) 487.